Boltzmann equation and Monte Carlo studies of electron transport in resistive plate chambers

2014 J. Phys. D: Appl. Phys. 47 435203

(http://iopscience.iop.org/0022-3727/47/43/435203)

IOP Publishing Journal of Physics D: Applied Physics

J. Phys. D: Appl. Phys. **47** (2014) 435203 (12pp) doi:10.1088/0022-3727/47/43/435203

Boltzmann equation and Monte Carlo studies of electron transport in resistive plate chambers

D Bošnjaković[1,2], Z Lj Petrović[1,2], R D White[3] and S Dujko[1]

[1] Institute of Physics, University of Belgrade, Pregrevica 118, 11070 Belgrade, Serbia
[2] Faculty of Electrical Engineering, University of Belgrade, Bulevar kralja Aleksandra 73, 11120 Belgrade, Serbia
[3] ARC Centre for Antimatter-Matter Studies, School of Engineering and Physical Sciences, James Cook University, 4811 Townsville, Australia

E-mail: dbosnjak@ipb.ac.rs

Received 18 June 2014, revised 25 August 2014
Accepted for publication 3 September 2014
Published 3 October 2014

Abstract

A multi term theory for solving the Boltzmann equation and Monte Carlo simulation technique are used to investigate electron transport in Resistive Plate Chambers (RPCs) that are used for timing and triggering purposes in many high energy physics experiments at CERN and elsewhere. Using cross sections for electron scattering in $C_2H_2F_4$, iso-C_4H_{10} and SF_6 as an input in our Boltzmann and Monte Carlo codes, we have calculated data for electron transport as a function of reduced electric field E/N in various $C_2H_2F_4$/iso-C_4H_{10}/SF_6 gas mixtures used in RPCs in the ALICE, CMS and ATLAS experiments. Emphasis is placed upon the explicit and implicit effects of non-conservative collisions (e.g. electron attachment and/or ionization) on the drift and diffusion. Among many interesting and atypical phenomena induced by the explicit effects of non-conservative collisions, we note the existence of negative differential conductivity (NDC) in the bulk drift velocity component with no indication of any NDC for the flux component in the ALICE timing RPC system. We systematically study the origin and mechanisms for such phenomena as well as the possible physical implications which arise from their explicit inclusion into models of RPCs. Spatially-resolved electron transport properties are calculated using a Monte Carlo simulation technique in order to understand these phenomena.

Keywords: resistive plate chambers, Boltzmann equation, Monte Carlo simulation, electron transport coefficients, negative differential conductivity

(Some figures may appear in colour only in the online journal)

1. Introduction

Resistive Plate Chambers (RPCs) are widely used particle detectors due to their simple construction, good detection efficiency, good spatial resolution and excellent timing resolution [1–6]. They are mainly utilized in large high-energy physics experiments for timing and triggering purposes [7–9] but they found their way into applications in other fields, including medical imaging [10, 11] and geophysics [12].

Depending on the applied electric field strength, geometry and gas mixture, RPCs can be operated in avalanche or streamer mode. The avalanche mode of operation provides a much better rate capability than streamer mode, but at the expense of smaller signals [5]. Typical gas mixtures used in the avalanche mode of operation are composed of tetrafluoroethane ($C_2H_2F_4$), iso-butane (iso-C_4H_{10}) and sulfur hexafluoride (SF_6). Tetrafluoroethane is a weakly electronegative gas with a high primary ionization. Iso-butane is a UV-quencher gas while sulfur hexafluoride is a strongly electronegative gas, used in avalanche mode to suppress the development of streamers. Recently, Abbrescia *et al* [13] have proposed new gaseous mixtures for RPCs that operate in

avalanche mode to overcome some of the problems encountered with standard gas mixtures based on tetrafluoroethane, iso-butane and sulfur hexafluoride.

There have been numerous models and simulations of RPCs. Being analytical [14, 15], Monte Carlo [3] or based on fluid equations [16–18], all macroscopic models rely on accurate data for electron swarm transport in gases. These quantities can be either measured in swarm experiments or calculated from electron impact cross sections by the Boltzmann equation analysis or by a Monte Carlo technique [19, 20]. In particle detector community, MAGBOLTZ [21] is the most commonly used Monte Carlo code for such a task. It has been routinely used many times in the past to evaluate electron transport data under the hydrodynamic conditions, and for different experimental arrangements including the Pulsed Townsend (PT) and steady-state Townsend conditions (SST). The motivation for this work lies with the fact that there are some important aspects of electron transport which cannot be analyzed by means of a Monte Carlo method used in MAGBOLTZ. One of these aspects includes the explicit and implicit effects of non-conservative collisions on electron transport and implications which arise from their inclusion in models of RPCs. Collisions in which the number of electrons changes either being produced or removed from the initial ensemble are regarded as non-conservative collisions. Typical examples of these collisions are ionization, attachment, as well as electron-induced detachment from negative ions and electron-ion recombination. These processes may have a marked influence on the electron transport properties and the detector performance. As an illustrative example, Doroud *et al* [22] have shown that the recombination dramatically reduces the amount of charge in the gas filled gap which in turn affects the rate capability in the multi gap RPC used for timing purposes in the ALICE experiment at CERN. In particular, kinetic phenomena induced by the explicit effects of ionization and/or electron attachment should be studied in terms of flux and bulk components of transport coefficients [19, 20, 23]. The distinction between these two sets of transport data has been systematically ignored in the particle detector community and reason for this might be the fact that MAGBOLTZ cannot be used to compute the bulk transport coefficients. At the same time the most accurate experiments used to unfold the cross section data measure bulk coefficients. However, the duality in transport coefficients is easy to understand physically. In this paper we present the required theoretical treatment of the non-conservative corrections, and highlight differences in origin and magnitudes of the bulk and flux transport coefficients for electrons in the gas mixtures used in RPCs in various high energy physics (HEP) experiments at CERN.

Recently, it was shown that the addition of SF_6 (and iso-C_4H_{10}) to standard RPC mixtures may improve several important aspects of the RPC performance in avalanche mode, including efficiency and time resolution [24]. It has been long established that electron attachment to SF_6 leads to the formation of both parent (SF_6^-) and fragment (SF_5^-, SF_4^-, SF_3^-, SF_2^-, F_2^- and F^-) negative ions [25]. In particular, the cross section for the creation of stable parent negative ions SF_6^- at zero energy is huge suggesting that the lower energy electrons are most likely to be consumed before their recombination with the positive ions. This in turn may induce some attachment induced kinetic phenomena in electron transport due to the strong electronegative nature of SF_6. One of the most striking phenomena induced by strong electron attachment in the mixtures of rare gases and fluorine is the negative absolute electron mobility [26, 27]. Occurrence of these phenomena should be carefully considered in numerical simulations in accordance with the experimental evaluation of the RPC performance.

Here we do not attempt to consider primary ionization effects, space charge effects and signal induction in the presence of resistive material nor do we attempt to compute the RPC performances, i.e. efficiency, time resolution and charge spectra. These important elements of modeling are the subject of our future publications [28]. Instead we isolate and investigate electron swarms under the action of a spatially uniform electric field. In the present work we solve the Boltzmann equation for electrons undergoing non-conservative collisions in the gas mixtures of $C_2H_2F_4$, iso-C_4H_{10} and SF_6 used in RPCs in various HEP experiments at CERN. In this application electron attachment and ionization play a key role in the electron behavior, therefore any modeling must treat them in a comprehensive manner. Variation and general trends of the mean energy and effective ionization coefficient, drift velocity and diffusion tensor with the applied reduced electric field are presented. We use our Monte Carlo simulation technique as a complementary method to Boltzmann's equation with the specific purpose to evaluate the spatially resolved transport data and distribution functions amidst non-conservative collisions. The knowledge of spatially resolved transport data is very useful in modeling of RPCs and understanding their performance. Fluid models of RPCs can be further improved by considering the non-local effects induced by a large spatial variation in the electric field during the avalanche-streamer transition or due to presence of physical boundaries. Correct implementation of transport data and accuracy of their calculation is also highlighted in the present work. Our methodology based on complementary Boltzmann and Monte Carlo studies of electron transport in neutral gases has already been used in different gas discharge problems [29]. This is the first paper to our knowledge where the combined Boltzmann equation analysis and Monte Carlo simulation technique are applied to the description of electron kinetics in the gas mixtures used in RPCs.

This paper is organized as follows. In section 2 we substantiate the existence of hydrodynamic regime and identify the differences in the bulk and flux transport coefficients. In section 2.1 we give a brief discussion of the theoretical multi term solution of the Boltzmann equation under non-conservative conditions. The basic elements of our Monte Carlo simulation code are discussed in section 2.2. In section 3, we present the results of a systematic study of electron transport in the gas mixtures used in RPCs that are used for timing and triggering purposes in many high energy experiments at CERN. We focus on the way in which the transport coefficients are influenced by non-conservative collisions, particularly by electron attachment. Spatially resolved energy and rate coefficients as well as spatial profiles of the electrons are calculated

by a Monte Carlo simulation technique with the aim of understanding the NDC and related phenomena. This paper represents the first comprehensive treatment of non-conservative electron transport in typical RPC gas mixtures based on a rigorous Boltzmann equation analysis and the Monte Carlo simulation technique.

2. Theoretical methods

Electron transport in non-conservative RPC gases should be analyzed in terms of bulk (e.g. reactive) and flux components. The main motivation for such analysis is to gain insight into the effect of non-conservative processes on electron transport as these processes influence many operating characteristics of the detector. For example, there is a direct link between the effective ionization coefficient and time resolution of an RPC. Spatial resolution, on the other hand, is greatly affected by transverse diffusion while the role of attachment processes is twofold. On one hand, electron attachment is a desirable process as it controls the avalanche multiplication and limits the amount of charge between the electrodes, which in turns improves the rate capability of an RPC. On the other hand, if the attachment is too strong with a large exponential decay rate for electrons then the time resolution and efficiency might be seriously affected. It is clear that care must be taken when non-conservative collisions are operative to ensure the optimal performance of the detector.

2.1. A brief sketch of the Boltzmann equation analysis

All information on the drift and diffusion of electrons in gases is contained in the electron phase-space distribution function $f(\mathbf{c}, \mathbf{r}, t)$, where $\mathbf{r}$ represents the spatial coordinate of an electron at time t, and $\mathbf{c}$ denotes its velocity. The distribution function $f(\mathbf{r}, \mathbf{c}, t)$ is evaluated by solving Boltzmann's equation:

$$\left(\partial_t + \mathbf{c}\cdot\nabla_{\mathbf{r}} + \frac{\mathrm{e}}{m}\mathbf{E}\cdot\nabla_{\mathbf{c}}\right) f(\mathbf{r}, \mathbf{c}, t) = -J(f, f_0) \ , \tag{1}$$

where ∂_t, $\nabla_{\mathbf{r}}$ and $\nabla_{\mathbf{c}}$ are the gradients with respect to time, space and velocity, while e and m are the charge and mass of the electron and $\mathbf{E}$ is the magnitude of the electric field. The right-hand side of (1) $J(f, f_0)$ denotes the linear electron-neutral molecule collision operator, accounting for elastic, inelastic and non-conservative (e.g. electron attachment and/or ionization) collisions, and f_0 is the velocity distribution function of the neutral gas (usually taken to be Maxwellian at fixed temperature). For elastic collisions we use the original Boltzmann collision operator [30], while for inelastic collisions we prefer the semiclassical generalization of Wang-Chang *et al* [31]. The collision operators for non-conservative collisions are discussed in [32, 33]. We assume that in the division of post-collision energy between the scattered and ejected electrons in an ionization process, all fractions are equally probable.

Solution of Boltzmann's equation (1) has been extensively discussed in our recent reviews [20, 34]. In brief, f is expanded in terms of normalized Burnett functions about a Maxwellian at an arbitrary temperature T_b. In the hydrodynamic regime, its space-time dependence is expressed by an expansion in terms of the gradient of the electron number density $n(\mathbf{r}, t)$. This assumption is generally valid for an RPC detector even in the regions where high energy particle creates the clusters of electrons with steep density gradients. One may expect that diffusion processes will act to validate the assumption on weak gradients after a certain period of time. Thus, the following expansion of the phase-space distribution function follows:

$$f(\mathbf{r}, \mathbf{c}, t) = \widetilde{\omega}(\alpha, c) \sum_{\nu=0}^{\infty} \sum_{l=0}^{\infty} \sum_{m=-l}^{l} \sum_{s=0}^{\infty} \sum_{\lambda=0}^{s} F(\nu lm|s\lambda;\alpha)\, \phi_m^{[\nu l]} G_m^{(s\lambda)} n(\mathbf{r}, t) \ , \tag{2}$$

where

$$\widetilde{\omega}(\alpha, c) = \left(\frac{\alpha^2}{2\pi}\right)^{3/2} \exp\left(-\frac{\alpha^2 c^2}{2}\right), \tag{3}$$

is a Maxwellian distribution function at a temperature T_b, with $\alpha^2 = \dfrac{m}{kT_\mathrm{b}}$. T_b is not equal to the neutral gas temperature and serves as a free and flexible parameter to optimize the convergence. The quantities $\phi_m^{[\nu l]}$ and $G_m^{(s\lambda)}$ are normalized Burnett functions and irreducible gradient tensor operator, respectively, and are defined in [32, 33]. The coefficients $F(\nu lm|s\lambda;\alpha)$ are called 'moments' and are related to the electron transport properties as detailed below. The bulk drift velocity (W), bulk diffusion coefficients (D_L, D_T) and effective ionization coefficient ($k_{\mathrm{eff\ ion}}$) are defined in terms of the diffusion equation and can expressed in terms of moments as follows [20, 34]:

$$W = \frac{\mathrm{i}}{\alpha} F(010|00) - \mathrm{i}n_0 \sum_{\nu'=1}^{\infty} J_{0\nu'}^0(\alpha)\, F(\nu'00|11) \ , \tag{4}$$

$$D_L = -\frac{1}{\alpha} F(010|11) - n_0 \left(\sum_{\nu'=1}^{\infty} J_{0\nu'}^0(\alpha)\, F(\nu'00|20) - \sqrt{2}\, F(\nu'00|20) \right), \tag{5}$$

$$D_T = -\frac{1}{\alpha} F(011|11) - n_0 \left(\sum_{\nu'=1}^{\infty} J_{0\nu'}^0(\alpha)\, F(\nu'00|20) + \frac{1}{\sqrt{2}} F(\nu'00|22) \right), \tag{6}$$

$$k_{\mathrm{eff\ ion}} = \mathrm{i}n_0 \sum_{\nu'=1}^{\infty} J_{0\nu'}^0(\alpha)\, F(\nu'00|00) \ , \tag{7}$$

where $J_{0\nu'}^0(\alpha)$ are reduced matrix elements of the collision operator. The bulk transport coefficients are the sum of the flux transport coefficients (defined in terms of Fick's law and given the first terms in each of the expressions (4)–(6)) and a contribution due to non-conservative collisions (the terms involving the summations in each expression). Differences between the two sets of coefficients thus arise when non-conservative processes are operative. The reader is referred to

[19, 20, 23, 34] for full details. Also of interest is the spatially homogeneous mean energy

$$\varepsilon = \frac{3}{2}kT_{\mathrm{b}}\left(1 - \sqrt{\frac{2}{3}}F\left(100|00\right)\right). \tag{8}$$

Using the above decomposition of f (2), the Boltzmann equation (1) is converted to a hierarchy of doubly infinite set of coupled algebraic equations for the moments. To obtain electron transport coefficients identified in (4)–(6) under conditions when the transport is greatly affected by non-conservative collisions, the index s in (2) must span the range (0–2) (e.g. second-order density gradient expansion). Solution of the system of equations can be found by truncation of the infinite summations in the velocity space representation in (2) at $l_{\max}$ and $\nu_{\max}$, respectively. The values of these indices required to achieve the designated convergence criterion, represent respectively the deviation of the velocity distribution from isotropy in velocity space, and the deviation from a Maxwellian speed distribution at the basis temperature T_{b}. The classical two term approximation sets $l_{\max} = 1$, which is not sufficient for molecular gases used in an RPC due to the anisotropy of f in velocity space. A value of $l_{\max} = 5$ was required for achieving an accuracy to within 1% . Depending of the basis temperature, values of $\nu_{\max} = 95$ were sometimes required under conditions when the distribution function was strongly non-equilibrium and far away from a Maxwellian. The resulting coefficient matrix is sparse and direct numerical inversion procedure is used to calculate the moments.

One should be aware of the differences in the definition of both sets of transport data, bulk and flux, and make sure that proper data are employed in the models. MAGBOLTZ is routinely used in particle detector community for determination of electron transport properties and few comments about this code are appropriate here. MAGBOLTZ cannot compute the bulk transport coefficients and it is exactly these data that are required for some aspects of modeling. For example, in the application of Legler's model for the avalanche size distribution as a function of the distance [2, 35], one should use the bulk drift velocity to evaluate the ionization coefficient. In addition, the bulk data should be generally used to unfold cross sections from experimentally measured and theoretically calculated transport coefficients [19, 20]. On the other, in fluid modeling of RPCs [16–18] the flux data should be generally used as an input although in some combined fluid/Monte Carlo models the bulk data are required. Generally speaking, the distinction between the bulk and flux data has been systematically ignored in the particle detector community and one of the principal aims of this work is to sound a warning to those who implement the swarm data to be aware of the origin of the transport data and the type of transport data required in their modeling. In this paper we illustrate that bulk and flux data may exhibit not only quantitative but also the qualitative differences in the mixtures of $C_2H_2F_4$, iso-C_4H_{10} and SF_6 used in RPCs operated in avalanche mode.

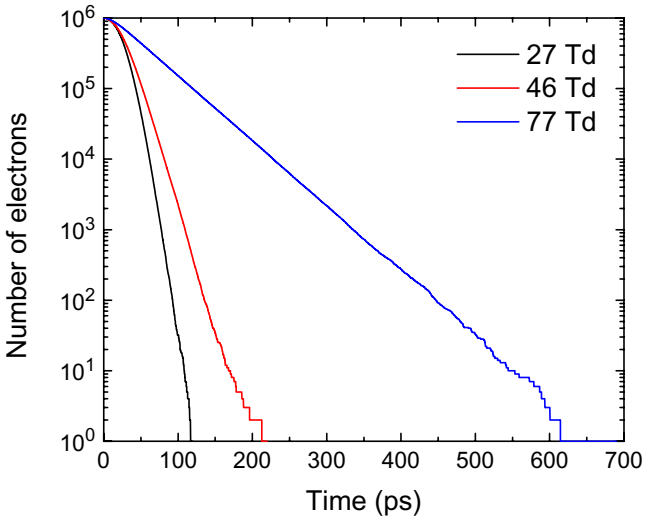

Figure 1. Exponential decay of the number of electrons for three different reduced electric fields as indicated on the graph. Calculations are performed for electrons in ALICE TOF RPC system.

2.2. A brief overview of our Monte Carlo simulation technique

Rather than present a full review of our Monte Carlo simulation technique, we highlight below some of its aspects associated with the sampling of spatially resolved electron transport data. In this work we apply the code primarily to calculate spatially resolved transport data with an aim of using these data to understand the sometimes atypical manifestations of the drift and diffusion in the RPCs. In order to sample spatially resolved transport parameters under hydrodynamic conditions, we have restricted the space to realistic dimensions of the RPC and divided it into cells. Every cell contains 100 sub-cells and these sub-cells are used to sample spatial parameters of electron swarm. This concept allowed us to follow the development of the swarm in both real space and normalized to 6σ, where σ is the standard deviation of the Gaussian distribution in space. The space (and time) resolved electron transport properties including the average energy/velocity and rate coefficients and also density profiles have been determined by counting the electrons and their energies/velocities as well as number of collisions in every cell.

When electron transport is greatly affected by non-conservative collisions, it is of key importance for a tractable simulation to efficiently control the number of electrons in simulations without distortion of the spatial gradients of the distribution function. It is well known that the statistical uncertainty of a Monte Carlo simulation decreases inversely with the square root of the number of electrons processed. In particular, when attachment occurs, electrons are lost continually, so that the number of electrons in the swarm decreases exponentially with time. This is illustrated in figure 1 for electrons in the gas mixture used in ALICE timing RPC.

The initial number of electrons is set to 1×10^6 and calculations are performed for a range of reduced electric fields E/N as indicated on the graph. We see that as E/N decreases the number of electrons decreases markedly. This is a consequence of an increasing collision frequency for electron attachment when E/N is reduced. In order to compensate

the electrons that are consumed by a strong attachment at low electron energy, the following rescaling procedure was adopted. First, the sampling time used for determination of various swarm dynamic properties (for example the mean position, velocity and energy of the electrons) was reduced and adjusted depending on the applied reduced electric field. Second, whenever electron is lost due to attachment another electron is randomly selected in its place from the ensemble of the remaining electrons. This was necessary in order to prevent large and continuous losses of electrons. This procedure was validated for a range of model and real gases when attachment is dominant non-conservative process and found to be correct [36, 37]. Other rescaling procedures to electron swarms with large exponential decay rates are available. The classical example is the procedure developed by Li *et al* [38]. The essence of their rescaling procedure is the addition of an artificial ionization channel with an energy-independent ionization frequency, chosen to be roughly equal to an attachment collision frequency for a given *E*/*N*. Similar procedure was applied to simulate electron transport in pure SF_6 by Yousfi *et al* [39]. Finally, we note that when ionization takes place the rescaling procedure was not necessary under conditions considered in this work, as ionization was not a sufficiently intensive process to increase the number of electrons beyond the limits set by the allocated memory.

3. Results and discussion

3.1. Preliminaries

As discussed in section 1, one of the aims of this work is to consider electron transport parameters as input in fluid and kinetic models of RPCs. The operating values of *E*/*N* for RPCs are above the critical electric fields for the corresponding gas mixtures, usually between 400 Td and 450 Td for timing RPC depending on the type of experiment and around 200 Td for triggering RPC. Fluid models of these detectors in both avalanche and streamer modes, however, require tabulation of transport data over a wide range of the reduced electric fields and/or mean energy of the electrons depending on the order of fluid approach [40, 41]. In this work we consider the reduced electric field range: 1–1000 Td (1Td = 1×10^{-21} Vm^2) while the pressure and temperature of the background gas are 1 atm and 293 K, respectively.

The cross sections for electron scattering from $C_2H_2F_4$ detailed in Šašić *et al* [42] are used in this study. The cross sections for electron scattering in iso-C_4H_{10} are taken from MAGBOLTZ code developed by Biagi. Finally, the cross sections for electron scattering in SF_6 are taken from Itoh *et al* [43]. Other sets of cross sections for electron scattering in these gases are available in the literature but our Boltzmann equation analysis has revealed that the present sets provide values of swarm parameters such as ionization and electron attachment rate coefficients, drift velocity, longitudinal and transverse diffusion coefficient in a good agreement with the experimental measurements for a wide range of *E*/*N* [44, 45]. The following mixtures are used for different RPCs considered in this work: (1) ALICE timing RPC $C_2H_2F_4$/iso-C_4H_{10}/SF_6 = 90/5/5 [8]; (2) ALICE triggering RPC $C_2H_2F_4$/iso-C_4H_{10}/SF_6 = 89.7/10/0.3 [8]; (3) CMS triggering RPC $C_2H_2F_4$/iso-C_4H_{10}/SF_6 = 96.2/3.5/0.3 [9]; and (4) ATLAS triggering RPC $C_2H_2F_4$/iso-C_4H_{10}/SF_6 = 94.7/5/0.3 [7].

3.2. Effects of non-conservative collisions

In the following sections we often find it necessary to refer to the explicit influence of electron attachment and/or ionization on electron transport to explain certain phenomena. The following elementary considerations apply. Even under the hydrodynamic conditions (far away from the boundaries, sources and sinks of electrons) the distribution of the average energy within the swarm is spatially anisotropic. This is illustrated in section 3.3 where spatially resolved average energy for electrons in ALICE timing RPC is shown as a function of *E*/*N*. Electrons at the front of the swarm generally have higher energy than those at the trailing edge, as on the average they have been accelerated through a larger potential. Since electron attachment and ionization are energy dependent, they will also occur with a spatial dependence. For example, if the collision frequency for electron attachment increases with energy, attachment will predominantly occur at the front of the swarm, resulting in a backwards shift of the swarm's centre of mass, which is observable as a reduction of the bulk drift velocity as compared with the flux drift velocity. The loss of high energy electrons also lowers the mean energy which in turns reduces the flux component of the diffusion. This process is known as *attachment cooling* [33].

If the collision frequency for electron attachment decreases with energy, then the opposite situation holds: the lower energy electrons at the trailing edge of the swarms will be consumed resulting in a forward shift of the swarm's centre of mass, which is observable as an increase of the bulk drift velocity. The mean energy is raised as the lower energy electrons are consumed resulting in an enhancement of the flux components of transverse and longitudinal diffusion. This phenomenon is known as *attachment heating* [32] and is particularly important for electron transport in the gas mixtures used in RPCs. Finally, when ionization takes place, electrons are preferentially created in regions of higher energy resulting in a shift in the centre of mass position as well as a modification of the spread about the centre of mass. This will be observable as an increase of the bulk drift velocity and the bulk diffusion coefficients. This situation also plays an important role in consideration of electron kinetics in RPCs analyzed in this work.

3.3. Boltzmann equation results for electron transport coefficients

In figure 2 we show the variation of mean energy with *E*/*N* for RPCs used in ALICE, CMS and ATLAS experiments at CERN.

The properties of the cross sections are reflected in the profiles of the mean energy and we observe three distinct regions of transport. Excepting ALICE timing RPC, in the remaining experiments we first observe a region of slow rise due to (relatively) large energy losses associated with vibrational

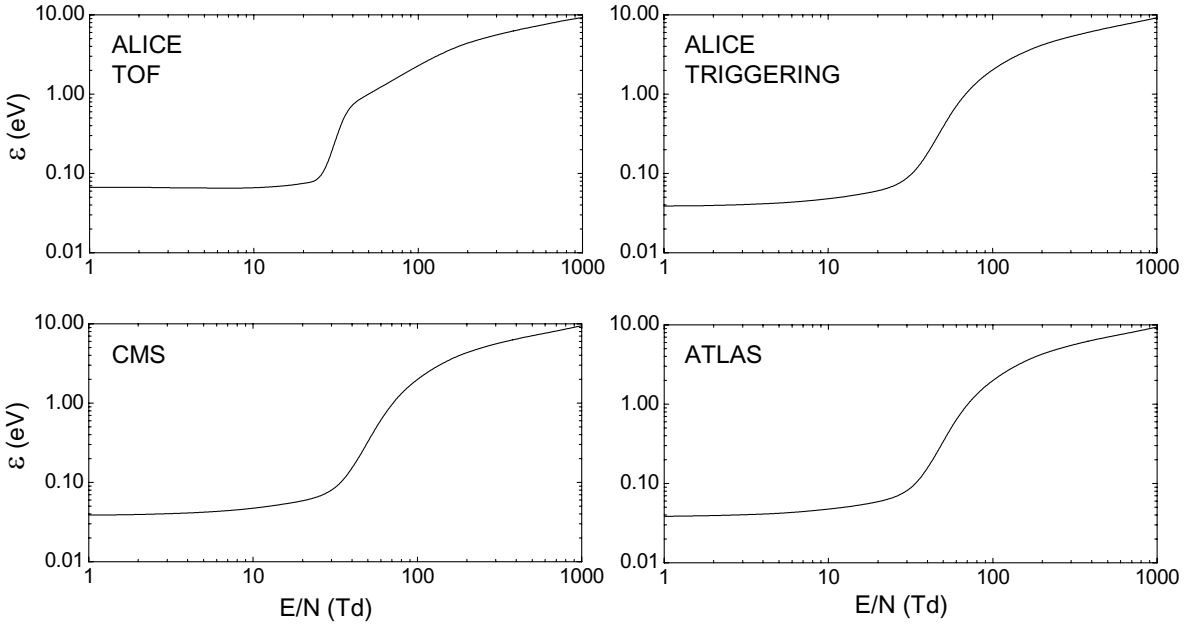

Figure 2. Variation of the mean energy with *E*/*N* for RPCs used in ALICE, CMS and ATLAS experiments at CERN.

excitations. Second, there is a region of sharp rise as the cross sections for vibrational excitations drop off and electrons start to gain energy from the electric field rapidly. Finally, there is another region of slow rise in the mean energy as new inelastic channels including the electronic excitation, neutral dissociation and ionization become open. The variation of the mean energy with *E*/*N* in these three RPCs systems is almost identical due to small differences in the abundances of $C_2H_2F_4$ and iso-C_4H_{10} in the gas mixtures. The amount of SF_6 in these systems is the same and set to 0.3%.

However, for ALICE timing RPC the situation is more interesting. In this system the amount of SF_6 in the gas mixture is much higher and the electron transport is greatly affected by electron attachment. In the limit of the lowest *E*/*N* considered in this work (less than 10 Td) and contrary to the results for other RPC systems, we see that for increasing *E*/*N* the mean energy varies very slowly and essentially stays unaltered. We also observe that the mean energy is significantly higher than thermal electron energy $\left(\frac{3}{2}kT\right)$ indicating the presence of an additional heating mechanism for electrons. This unusual situation follows from the combined effects of attachment heating and inelastic cooling. The term *inelastic cooling* simply refers to the fact that whenever an electron undergoes an inelastic collision it loses at least the threshold energy of the excitation process and emerges from the collision with reduced energy. In the energy range of interest, the collision frequency for electron attachment (which leads to the formation of stable parent SF_6^- negative ion) decreases with the electron energy and the lower energy electrons which predominantly exist at the trailing edge of the swarm are preferentially consumed. As already discussed in section 3.2, under these conditions the mean energy is raised and bulk drift velocity is increased (see figure 3). However, due to inelastic cooling if the electrons have energy just above the threshold energy, then in any inelastic encounter with a neutral they will lose almost all energy, resulting in a substantial cooling effect on the swarm, even if only a relatively small fraction of the electrons have the required energy. This is exactly what happens for electrons in ALICE timing RPC; due to attachment heating the mean energy is raised above thermal energy and due to inelastic cooling the mean energy cannot be further increased for increasing *E*/*N* as the collision frequency for inelastic collisions in this energy range rapidly increases with the electron energy.

In figure 3 we show the variation of the bulk and flux drift velocity with *E*/*N* for RPCs used in ALICE, CMS and ATLAS experiments at CERN. In all experiments the bulk component dominates the flux component over the entire *E*/*N* range consider in this work. For lower *E*/*N* this follows from the attachment heating while for higher *E*/*N* this is a consequence of the explicit effects of ionization on the drift velocity. The effects of electron attachment are stronger than those induced by ionization and are the most evident for ALICE timing RPC where differences between the bulk and flux values are of the order of 100% for lower *E*/*N*. For other RPC systems these differences are of the order of 10% for lower *E*/*N* while for higher *E*/*N* are around 20%.

The existence of negative differential conductivity (NDC) in the bulk drift velocity component with no indication of any NDC for the flux component in the ALICE timing RPC system is certainly one of the most striking phenomena observed in this work. NDC is a kinetic phenomenon which represents the decrease of the drift velocity with increasing driving electric field. From the plot of the drift velocity for ALICE timing RPC it is seen that electrons exhibit NDC in the bulk drift velocity for reduced electric fields between 30 Td and 100 Td. Conditions leading to this phenomenon have been extensively discussed by Petrović *et al* [46] and Robson [47]. In brief, it was concluded that NDC arise from certain combination of

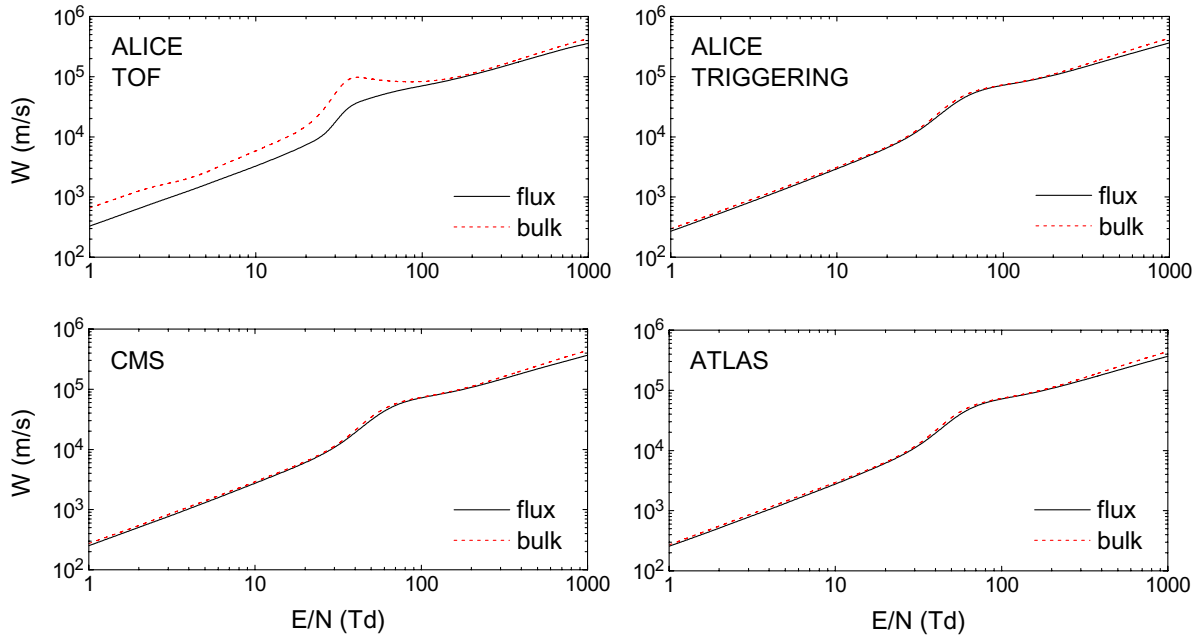

Figure 3. Variation of the bulk and flux drift velocities with *E*/*N* for RPCs used in ALICE, CMS and ATLAS experiments at CERN.

elastic-inelastic cross sections and is present in both the bulk and flux drift velocity components. The conditions for the attachment or ionization (non-conservative collision) induced NDC were first discussed by Vrhovac and Petrović [48] where it was concluded that the effect is possible but most likely to result in both bulk and flux drift velocities albeit at a different degree. This paper left a possibility that the flux drift velocity may not have NDC but a strongly developed plateau indicating that the NDC is on verge of being observable. This conclusion was based on the survey of observable effects for most gases with strong dissociative attachment.

In our case, however, NDC is present only in the bulk drift velocity which is a reminiscent of recently observed NDC effect for positrons in molecular gases [49, 50]. In these studies, it was concluded that NDC is induced by non-conservative nature of Positronium (Ps) formation. This conclusion has been confirmed in calculations where the Ps formation was treated as a conservative inelastic process; the NDC phenomenon has been removed from the profiles of the bulk drift velocity along with the differences between bulk and flux drift velocity components. Following the same strategy, we have treated electron attachment as a conservative inelastic process for SF_6 in our Boltzmann equation analysis. Results of our calculations are shown in figure 4. We see that NDC is absent from the profile of the bulk drift velocity and the only differences between the bulk and flux drift velocity are those originating from the explicit contribution of ionization for *E*/*N* higher than approximately 200 Td. The physical mechanisms behind the attachment induced NDC phenomenon is discussed in section 3.4.

In figures 5 and 6 we show the variation of the longitudinal and transverse diffusion coefficients with *E*/*N* for RPCs used in ALICE, CMS and ATLAS experiments at CERN. Both the bulk and flux values are shown and we see that all diffusion

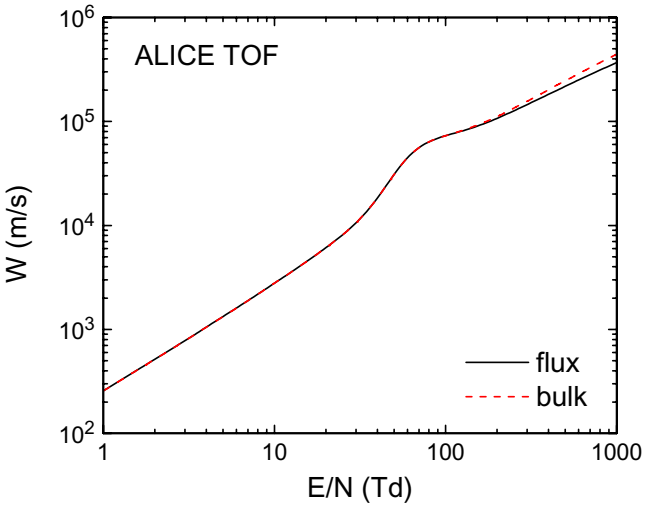

Figure 4. Variation of the bulk and flux drift velocity with *E*/*N* when electron attachment is treated as a conservative inelastic process for electrons in an ALICE timing RPC.

coefficients reflect to some degree the three distinct regions of electron transport discussed above. For ALICE triggering, CMS and ATLAS RPC systems, the variations of bulk and flux components of ND_L and ND_T with *E*/*N* are almost identical. Differences between the bulk and flux data for ND_L and ND_T are of the order of 20% . In these systems the differences between the bulk and flux values are only of quantitative nature and are not as high as those present between the bulk and flux values for ND_L and ND_T in the ALICE timing RPC system. In this case the bulk and flux components of the diffusion coefficients exhibit *qualitatively* different behavior; although as *E*/*N* increases both ND_L and ND_T generally increase, there exist certain regions of *E*/*N* where the bulk components of both ND_L and ND_T (and flux ND_L) are decreased for increasing *E*/*N*.

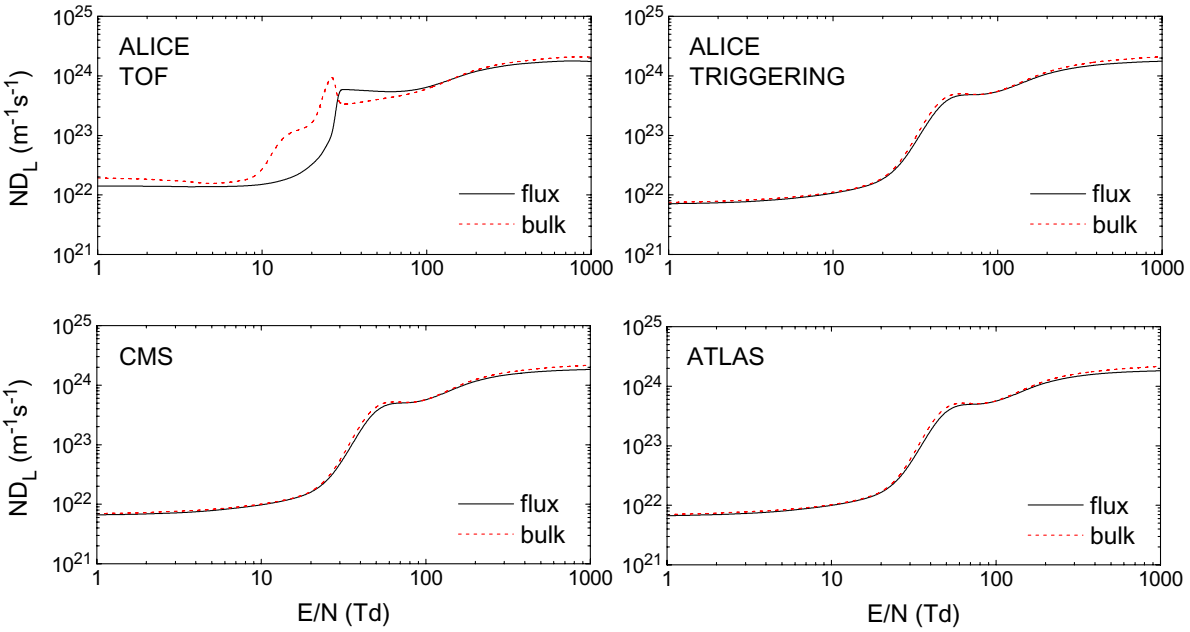

Figure 5. Variation of the longitudinal diffusion coefficient with *E*/*N* for RPCs used in ALICE, CMS and ATLAS experiments at CERN. Dashed lines are bulk coefficients while solid lines represent flux coefficients.

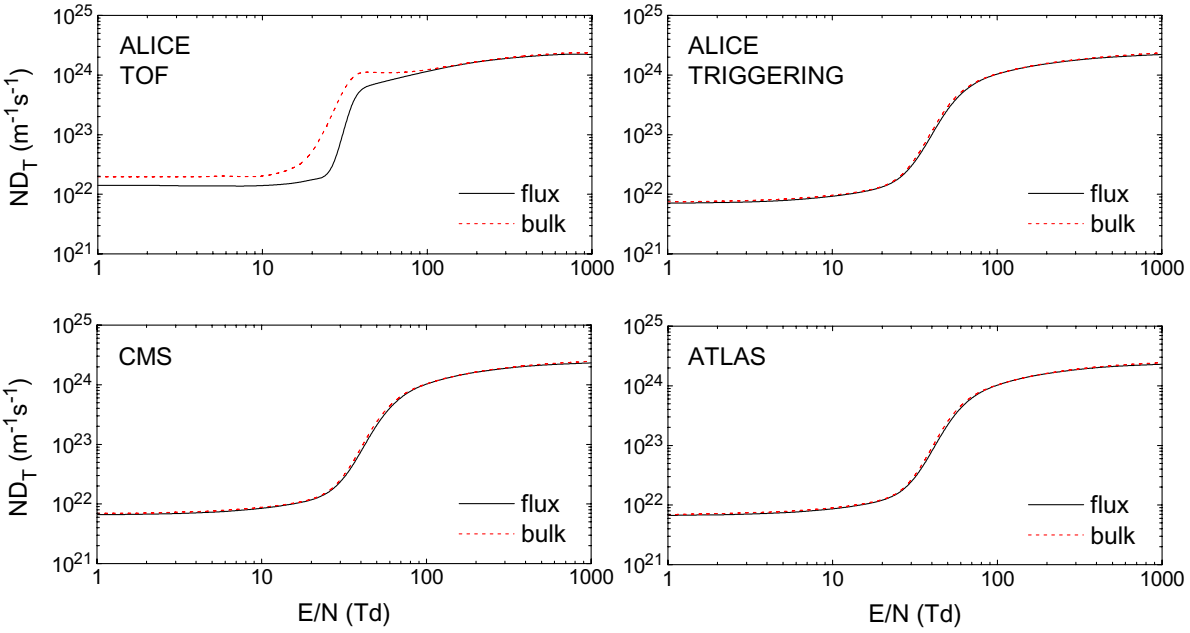

Figure 6. Variation of the transverse diffusion coefficient with *E*/*N* for RPCs used in ALICE, CMS and ATLAS experiments at CERN. Dashed lines are bulk coefficients while solid lines represent flux coefficients.

This illustrates the complexity of diffusion processes in general and for electrons in RPC systems at CERN indicating how difficult it is to understand the influence of non-conservative collisions on the diffusion coefficients. In brief, many parallel factors affect the diffusion simultaneously. In addition to the effects of thermal anisotropy (dispersion of electrons due to thermal motion is not the same in different directions) and anisotropy at elevated reduced electric fields (spatial variation of the average energy in conjunction with energy-dependent collision frequency produces differences in the average local velocities for a given direction, which act to inhibit and/or enhance diffusion in that direction), there is always the contribution of non-conservative collisions and the complex energy dependence of electron attachment and ionization that even further complicate the physical picture. In conclusion, our results suggest a weak sensitivity of the diffusion coefficients with respect to electron attachment and ionization for ALICE triggering, CMS and ATLAS RPC systems and a much more complex behavior of diffusion processes for electrons in ALICE timing RPC.

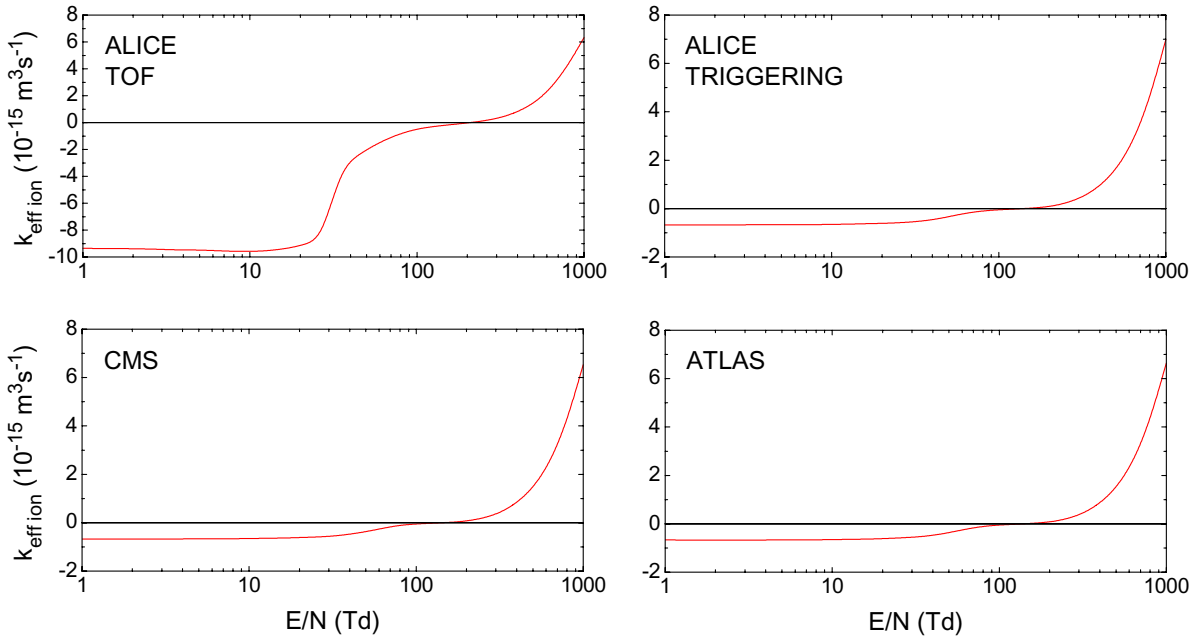

Figure 7. Variation of the effective ionization coefficient with *E*/*N* for RPCs used in ALICE, CMS and ATLAS experiments at CERN.

In figure 7 we show the variation of the effective ionization coefficient with *E*/*N* for RPCs used in ALICE, CMS and ATLAS experiments at CERN. The variation of this property with *E*/*N* is almost identical for ALICE triggering, CMS and ATLAS RPC systems due to small variations in the abundances of $C_2H_2F_4$ and iso-C_4H_{10} in the gas mixtures. The critical electric field for these systems is around 140 Td. The critical electric field for ALICE timing RPC is much higher, around 215 Td, due to higher abundance of SF_6 in the gas mixture and stronger effects of electron attachment on the electron energy distribution function.

3.4. Monte Carlo results for spatially resolved transport data and distribution function

While all results presented above may reproduced exactly (for all practical purposes) by Monte Carlo simulation (albeit with a much more computing effort) there is a number of results important for RPC modeling that may be obtained by Monte Carlo technique with less difficulty and a more direct interpretation. In this section we show spatially resolved electron transport data that are sampled at every location over the entire swarm. The effect of the electric field on the spatial distribution of the electron transport data and distribution function is examined. In figure 8 we show the spatial profile and spatially resolved average energy for four different values of *E*/*N* as indicated in the graphs. The Monte Carlo simulations were simplified by assuming stationary gas (T = 0 K). This is the reason why our Monte Carlo results for electron transport coefficients are slightly shifted to the left, towards lower *E*/*N* comparing to our Boltzmann equation results obtained for the gas temperature of 293 K (not shown here). As a consequence, according to our Monte Carlo simulations the NDC occurs approximately between 20 Td and 77 Td while the Boltzmann equation analysis suggest the NDC between 30 Td and 100 Td. One should bear this in mind in the following discussions.

In addition to our actual results given by solid lines where electron attachment is treated as a true non-conservative process, the results denoted by the dashed lines are obtained assuming electron attachment as a conservative inelastic process with zero energy loss. When electron attachment is treated as a conservative inelastic process, the spatial profile of electrons is almost perfectly symmetric and it has a typical Gaussian profile independently of the applied *E*/*N*. The spatially resolved average energy has a characteristic slope indicating spatially anisotropic distribution of the electron energy. There are no imprinted oscillations in the spatial profile of the electrons or in the profile of the average energy indicating the collisional energy loss is governed essentially by 'continuous' energy loss processes [51].

When electron attachment is treated regularly, as a true non-conservative process, we observe dramatic modifications to the spatial profile of the electron density and to the spatially resolved average energy. For *E*/*N* of 5.9 Td and 10 Td the spatial profile of electrons is no longer Gaussian while for *E*/*N* of 21 Td the spatial profile exhibits an asymmetric Gaussian distribution whose height is significantly decreased comparing to the Gaussian profile of the swarm when electron attachment is treated as a conservative inelastic process. For *E*/*N* = 5.9 Td we see that the average energy is essentially spatially uniform along the swarm. This is indicative of our normalization procedure: the spatial profile is not symmetric and number of electrons attachments is also asymmetric along the swarm and combination of these two yields a little spatial variation of the average energy along the swarm. For *E*/*N* = 10 Td, however, we observe that the trailing edge of the swarm is drastically cut off while the average energy remains

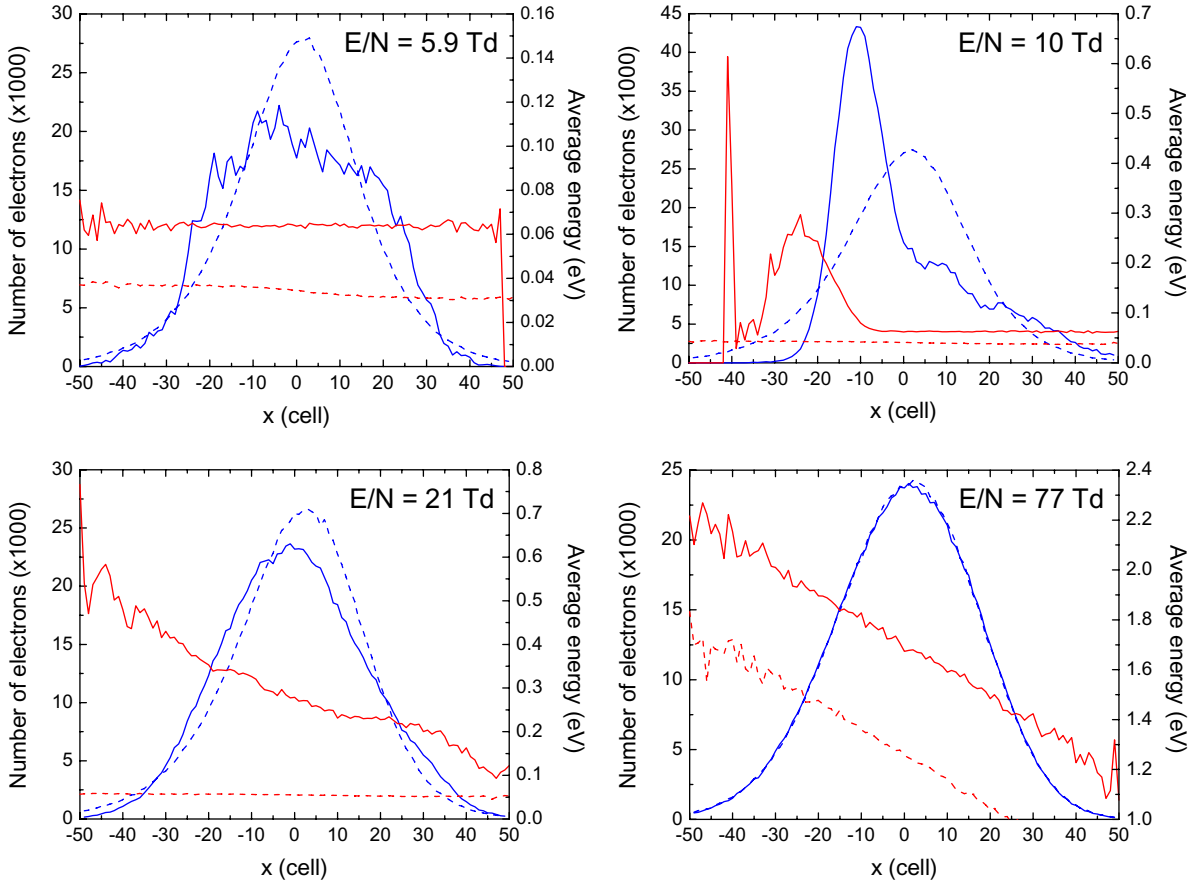

Figure 8. Spatial profile of electrons (blue curves) and spatially resolved averaged energy (red curves) at four different *E*/*N* in ALICE timing RPC. Full lines denote the results when electron attachment is treated as a non-conservative process, while the dashed lines represent our results when electron attachment is treated as a conservative inelastic process. (t = 1 ns).

essentially constant otherwise. At the leading edge of the swarm, the average energy is raised with a much steeper slope towards the front. Before reaching the highest energy at the leading edge of the swarm, there is a spatial region where the average energy is first drastically decreased, and then rapidly increased in a very narrow spatial region. For *E*/*N* = 21 Td the spatial dependence of the average energy is almost linear and no sharp jumps and drop-offs in the profile are observed. For increasing *E*/*N* the average electron energy increases and there are fewer and fewer electrons available for attachment. Thus the explicit contribution of electron attachment is further reduced which in turns removes the differences between the bulk and flux components of the drift velocity and diffusion coefficients in the energy region where NDC occurs. Finally for *E*/*N* = 77 Td, the spatial profile of electrons almost coincides with the profile obtained under conditions when electron attachment is treated as a conservative inelastic process. In both cases the average energy linearly increases from the trailing edge towards the leading part of the swarm. This is regime when electron attachment has no longer dominant control over the electron swarm behavior.

The spatially resolved attachment rates are shown in figure 9 and are calculated under the same conditions as for the spatial profile of the electrons and spatially averaged energy. They have complex profiles that reflect the overlap of the average energy and the corresponding cross sections. The

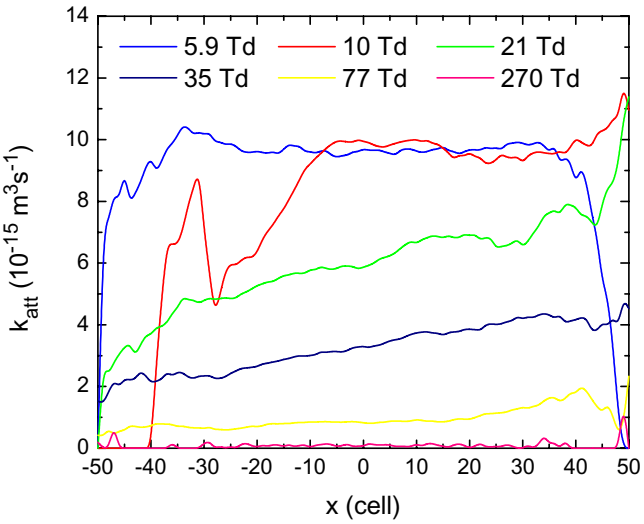

Figure 9. Spatially resolved attachment rate coefficient for a range of *E*/*N* in ALICE timing RPC. (t = 1 ns).

attachment rate is generally higher at the trailing edge of the swarm where the average energy of the electrons is lower and exactly these lower energy electrons are most likely to be consumed by electron attachment. This results in a forward shift of the centre of mass of the electron swarm, which is observable as an increase of the bulk drift velocity over the flux

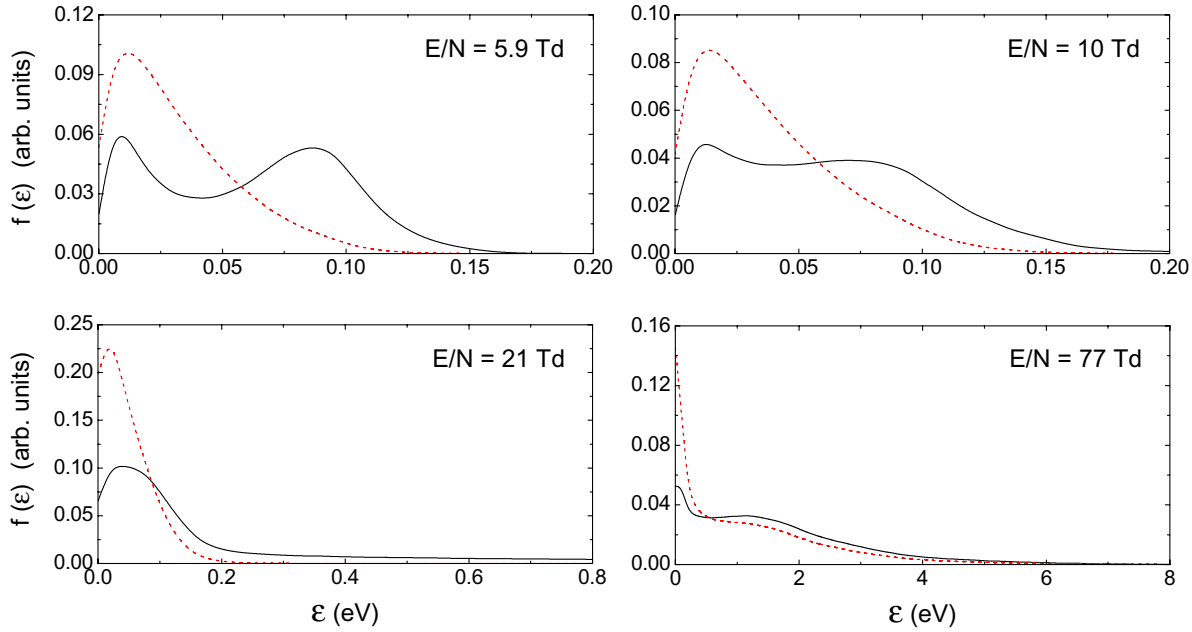

Figure 10. Electron energy distribution functions for four different *E*/*N* in ALICE timing RPC. Black lines denote the results when electron attachment is treated as non-conservative process while dashed red lines represent our results when electron attachment is treated as a conservative inelastic process. (t = 1 ns).

values as discussed above. For increasing *E*/*N* the spatially resolved rate coefficients are decreased suggesting much less impact of electron attachment on the electron swarm behavior.

When electron transport is greatly affected by non-conservative collisions it is often very useful to look at the energy distribution functions in order to make conclusions about the underlying physics of some processes. In figure 10 we show the electron energy distribution functions for the same four values of *E*/*N* considered above. The electron energy distribution functions are calculated when electron attachment is treated regularly as a true non-conservative process (black line) and under conditions when electron attachment is assumed to be a conservative inelastic process (dash red line). We see that strong electron attachment induces a 'hole burning' in the electron energy distribution function. For decreasing *E*/*N* the electron energy is generally reduced and the attachment cross section becomes larger. As a result the effect of electron loss on the distribution function increases. This phenomenon has been extensively discussed for electrons in O_2 [52] and O_2 mixtures [29, 53] and under conditions leading to the phenomenon of absolute negative electron mobility [26, 27]. The same effect is not present when attachment is treated as a conservative inelastic process. Under these conditions, we see that the population of low energy electrons is much higher than the corresponding situation when electron attachment is treated regularly. For increasing *E*/*N*, the population of high energy electrons becomes well described even when electron attachment is treated as a conservative inelastic process.

4. Conclusion

In this work, we have presented the results of a systematic investigation of non-conservative electron transport in the mixtures of $C_2H_2F_4$, iso-C_4H_{10} and SF_6 used in RPCs in ALICE, CMS and ATLAS experiments at CERN. We have considered conditions consistent with the electrons in an avalanche and streamer mode of operation of these RPC systems with partial motivation being the provision of transport coefficients to be employed in fluid modeling of such systems. Transport coefficients presented in this work are given as a function of *E*/*N* and are accurate to within 2% . The *E*/*N*-dependence of electron transport coefficients for ALICE triggering, CMS and ATLAS RPC systems are almost identical due to similar composition of the corresponding gas mixtures. The bulk drift velocity is slightly higher than flux component even for lower *E*/*N* indicating the presence of attachment heating. When ionization dominates attachment the difference between the bulk and flux drift velocities is further increased. The most striking phenomenon observed in this work is the existence of NDC in the bulk drift velocity component with no indication of any NDC for the flux component in the ALICE timing RPC system. This phenomenon was predicted as possible [48] but has never been observed for electrons primarily as the dominance of explicit effects and strongly energy dependent attachment were sought due to limitations of the momentum transfer theory that was employed in that paper. In order to understand the physical mechanisms behind of this atypical manifestation of the drift velocity, we have calculated spatially resolved transport properties and energy distribution functions for electric fields critical for occurrence of this phenomenon. It was found that the attachment heating governs the phenomenon and plays the dominant role in consideration of non-conservative effects on various transport properties. A 'hole burning' in the distribution function has been observed illustrating the richness and complexity of electron transport phenomena in RPCs.

Acknowledgments

DB, ZLjP and SD acknowledge support from MPNTRRS Projects OI171037 and III41011. RDW is supported by the Australian Research Council.

References

[1] Santonico R and Cardarelli R 1981 *Nucl. Instrum. Methods* **187** 377–80
[2] Riegler W, Lippmann C and Veenhof R 2003 *Nucl. Instrum. Methods* A **500** 144–62
[3] Riegler W and Lippmann C 2004 *Nucl. Instrum. Methods* A **518** 86–90
[4] Santonico R 2012 *Nucl. Instrum. Methods* A **661** S2–5
[5] Fonte P 2002 *IEEE Trans. Nucl. Sci.* **49** 881–7
[6] Fonte P 2013 *J. Instrum.* **8** P11001
[7] The ATLAS Collaboration 2008 *J. Instrum.* **3** S08003
[8] The ALICE Collaboration 2008 *J. Instrum.* **3** S08002
[9] The CMS Collaboration 2008 *J. Instrum.* **3** S08004
[10] Blanco A, Couceiro M, Crespo P, Ferreira N C, Ferreira Marques R, Fonte P, Lopes L and Neves J A 2009 *Nucl. Instrum. Methods* A **602** 780–3
[11] Couceiro M, Crespo P, Mendes L, Ferreira N, Ferreira Marques R and Fonte P 2012 *Nucl. Instrum. Methods* A **661** S156–8
[12] Cârloganu C *et al* 2013 *Geosci. Instrum. Methods Data Syst.* **2** 55–60
[13] Abbrescia M, Cassano V, Nuzzo S, Piscitelli G, Vadruccio D and Zaza S 2012 *Nucl. Instrum. Methods* A **661** S190–3
[14] Riegler W 2009 *Nucl. Instrum. Methods* A **602** 377–90
[15] Mangiarotti A, Fonte P and Gobbi A 2004 *Nucl. Instrum. Methods* A **533** 16–21
[16] Khosravi Khorashad L, Moshaii A and Hosseini S 2011 *Europhys. Lett.* **96** 45002
[17] Khosravi Khorashad L, Eskandari M and Moshaii A 2011 *Nucl. Instrum. Methods* A **628** 470–3
[18] Moshaii A, Khosravi Khorashad L, Eskandari M and Hosseini S 2012 *Nucl. Instrum. Methods* A **661** S168–71
[19] Petrović Z Lj, Dujko S, Marić D, Malović G, Nikitović Ž, Šašić O, Jovanović J, Stojanović V and Radmilović-Rađenović M 2009 *J. Phys. D: Appl. Phys.* **42** 194002
[20] White R D, Robson R E, Dujko S, Nicoletopoulos P and Li B 2009 *J. Phys. D: Appl. Phys.* **42** 194001
[21] Biagi S F 1999 *Nucl. Instrum. Methods* A **421** 234–40
[22] Doroud K, Afarideh H, Hatzifotiadou D, Rahighi J, Williams M C S and Zichichi A 2009 *Nucl. Instrum. Methods* A **610** 649–53
[23] Robson R E 1991 *Aust. J. Phys.* **44** 685
[24] Lopes L, Fonte P and Mangiarotti A 2012 *Nucl. Instrum. Methods* A **661** S194–7
[25] Christophorou L G and Olthoff J K 2000 *J. Phys. Chem. Ref. Data* **29** 267
[26] Dyatko N A, Napartovich A P, Sakadzic S, Petrovic Z and Raspopovic Z 2000 *J. Phys. D: Appl. Phys.* **33** 375–80
[27] Dujko S, Raspopovic Z M, Petrovic Z L and Makabe T 2003 *IEEE Trans. Plasma Sci.* **31** 711–6
[28] Bošnjaković D, Petrović Z Lj and Dujko S 2014 A microscopic Monte Carlo approach in modeling of resistive plate chambers *J. Instrum.* submitted
[29] Dujko S, Ebert U, White R D and Petrović Z Lj 2011 *Japan. J. Appl. Phys.* **50** 08JC01
[30] Boltzmann L 1872 *Wien. Ber.* **66** 275
[31] Wang-Chang C S, Uhlenbeck G E and de Boer J 1964 *Studies in Statistical Mechanics* **2** (New York: Wiley) p 241
[32] Robson R E and Ness K F 1986 *Phys. Rev.* A **33** 2068–77
[33] Ness K F and Robson R E 1986 *Phys. Rev.* A **34** 2185–209
[34] Dujko S, White R D, Petrović Z Lj and Robson R E 2010 *Phys. Rev.* E **81** 046403
[35] Legler W 1961 *Z. Naturf.* **16a** 253
[36] Raspopović Z M, Sakadžić S, Bzenić S A and Petrović Z Lj 1999 *IEEE Trans. Plasma Sci.* **27** 1241–8
[37] Petrović Z Lj, Raspopović Z M, Dujko S and Makabe T 2002 *Appl. Surf. Sci.* **192** 1–25
[38] Li Y M, Pitchford L C and Moratz T J 1989 *Appl. Phys. Lett.* **54** 1403
[39] Yousfi M, Hennad A and Alkaa A 1994 *Phys. Rev.* E **49** 3264–73
[40] Dujko S, Markosyan A H, White R D and Ebert U 2013 *J. Phys. D: Appl. Phys.* **46** 475202
[41] Markosyan A H, Dujko S and Ebert U 2013 *J. Phys. D: Appl. Phys.* **46** 475203
[42] Šašić O, Dupljanin S, de Urquijo J and Petrović Z Lj 2013 *J. Phys. D: Appl. Phys.* **46** 325201
[43] Itoh H, Matsumura T, Satoh K, Date H, Nakao Y and Tagashira H 1993 *J. Phys. D: Appl. Phys.* **26** 1975–9
[44] Bošnjaković D, Dujko S, Petrović Z Lj 2012 Electron transport coefficients in gases for resistive plate chambers *Proc. of the 26th Summer School and Int. Symp. on the Physics of Ionized Gases* (Zrenjanin, Serbia, 27–31 August) Kuraica M and Mijatović Z (Bristol: IOP) pp 265–8
[45] Bošnjaković D, Petrović Z Lj and Dujko S 2013 Monte Carlo modelling of resistive plate chambers *Proc. of the XVII Int. Workshop on Low-Energy Positron and Positronium Physics and the XVIII Int. Symposium on Electron-Molecule Collisions and Swarms* (Kanazawa, Japan, 19–21 July) p 44
[46] Petrović Z Lj, Crompton R W and Haddad G N 1984 *Aust. J. Phys.* **37** 23
[47] Robson R E 1984 *Aust. J. Phys.* **37** 35
[48] Vrhovac S B and Petrović Z Lj 1996 *Phys. Rev.* E **53** 4012–25
[49] Banković A, Dujko S, White R D, Marler J P, Buckman S J, Marjanović S, Malović G, García G and Petrović Z Lj 2012 *New J. Phys.* **14** 035003
[50] Banković A, Dujko S, White R D, Buckman S J and Petrović Z Lj 2012 *Nucl. Instrum. Methods* B **279** 92–5
[51] Dujko S, White R D, Raspopović Z M and Petrović Z Lj 2012 *Nucl. Instrum. Methods* B **279** 84–91
[52] Skullerud H R 1983 *Aust. J. Phys.* **36** 845
[53] Hegerberg R and Crompton R W 1983 *Aust. J. Phys.* **36** 831